DOI:10.1021/jf103312t

JOURNAL OF AGRICULTURAL AND FOOD CHEMISTRY
ARTICLE

Formation and Stability of Nanofibers from a Milk-Derived Peptide

Marie-Michèle Guy,[†] Mélanie Tremblay,[§] Normand Voyer,[§] Sylvie F. Gauthier,[†] and Yves Pouliot*,[†]

[†]STELA Dairy Research Center, Institute of Nutraceuticals and Functional Foods (INAF) and [§]PROTEO Protein Structure, Function and Engineering Research Network, Département de chimie, Université Laval, Quebec City, QC, Canada G1V 0A6

The objective of the present work was to investigate the physicochemical conditions that trigger the self-assembly of peptide β-lg f1−8 and therefore lead to nanofibers and hydrogel formation. Nanostructures formed by self-assembly of peptide β-lg f1−8 in the pH range of 2.0−11.0 were studied by transmission electron microscopy (TEM). Hydrogel formation was studied as a function of pH and resulted in evidence of a link between hydrogel formation and the charge distribution carried by the peptide structure. Finally, circular dichroism (CD) spectroscopy was used to characterize the effects of peptide concentration (0.4−2.0 mg/mL), ionic strength (0−1 M NaCl), and temperature (20−80 °C) on the secondary structure of peptide β-lg f1−8. Hydrogels were obtained at peptide concentrations above 2.5 mg/mL. Peptide concentration and pH adjustment were shown to trigger self-assembly of β-lg f1−8, but increasing ionic strength had no effect. Heating to 80 °C induced a stronger CD signal intensity due to an increase in solubility of the peptide, whereas only slight changes in CD pattern were found upon cooling to 20 °C. Overall, results emphasize the role of particular molecular interactions in β-sheet self-assembly of peptide β-lg f1−8 and pH-dependent electrostatic interactions occurring between β-lg f1−8 units, which can explain its propensity to self-assembly.

KEYWORDS: Milk peptide; self-assembly; β-sheet; nanofibers; hydrogel; secondary structure; circular dichroism

INTRODUCTION

Research on the self-organization properties of peptides is an active and diverse field, which applies to many areas from biomedicine and biotechnology to material science and nanotechnology (*1*). Several studies have demonstrated that hydrogels formed of self-assembling peptides are especially suitable for various biomedical applications, such as scaffolds for encapsulation and injection of cells in vivo (*2*), matrices for neuronal cell attachment (*3*), scaffolds for tooth enamel remineralization (*4*), and delivery vehicles for heparin (*5*). Moreover, some neurodegenerative diseases (including Alzheimer's, Parkinson's, and Creutzfeldt−Jacob diseases) are associated with the formation of protein aggregates in the brain caused by self-assembly of polypeptides into amyloid fibrils. Therefore, short self-assembling peptides are useful model systems to study the molecular mechanism underlying amyloid fibril formation (*6*).

Peptide self-assembly is a type of aggregation by which several individual entities of a peptide form well-defined nanostructures stabilized via noncovalent interactions, most importantly hydrophobic interactions and hydrogen bonds. Several studies have highlighted the relationship between peptide self-assembly and secondary structure transition to β-sheet conformation (*2*, *7*−*14*). Likewise, several papers have described peptide self-assembly leading to the formation of discrete nanostructures, nanotubes, nanofibers, and hydrogels (*15*, *16*).

Most of the self-assembling peptides reported in the literature consist of synthetic amphiphilic peptides specially designed with one of the motifs that typically form β-sheets, which consist of alternating hydrophobic and hydrophilic residues (*15*). Interestingly, some authors have also reported on molecular self-assembly occurring with peptide mixtures that result from the hydrolysis of milk proteins.

Ipsen et al. (*17*) have shown that limited hydrolysis of α-lactalbumin (α-la) by a protease from *Bacillus licheniformis* (BLP) leads to peptide aggregation through self-assembly, which results in the formation of gels that exhibit a uniform tubular microstructure. In a previous study (*18*), it was demonstrated that the peptide β-lg f1−8, contained in a tryptic hydrolysate of β-lactoglobulin (β-lg), acts as the driving force of an aggregation phenomenon resulting from an efficient β-sheet self-assembly process. Peptide β-lg f1−8 is released from enzymatic hydrolysis (trypsin) of the N-terminal extremity of β-lg and has the amino acid sequence LIVTQTMK. This peptide is amphiphilic, with a hydrophobic part located at the N-terminus and a hydrophilic lysine residue at the C-terminus. This peptide was shown to

*Author to whom correspondence should be addressed [phone (418) 656-5988; fax (418) 656-3353; e-mail Yves.Pouliot@inaf.ulaval.ca].

 Published on Web 12/23/2010

undergo self-assembly by a secondary structure transition from random coils to β-sheet conformation occurring in the pH range of 9.0−11.0 (*18*).

The aim of the present work was to investigate the physicochemical conditions that trigger self-assembly of peptide β-lg f1−8, which leads to nanofiber formation. Nanostructures formed by self-assembly of peptide β-lg f1−8 were studied using transmission electron microscopy (TEM) at different pH values. We also compared changes in nanostructure morphology to conformation changes in the secondary structure of the peptide induced as a function of pH and determined by circular dichroism (CD) spectroscopy measurements. Finally, the effects of peptide concentration, temperature, ionic strength, and buffer composition on the secondary structure adopted by peptide β-lg f1−8 were characterized by CD measurements.

MATERIALS AND METHODS

Peptide Isolation and Purification. Peptide β-lg 1−8 was prepared as previously described (*18*). Briefly, flocculated tryptic hydrolysate of β-lg was rehydrated to 5% (w/v) in HPLC-grade water and centrifuged at 5000*g* for 12 min at room temperature. The precipitate was resuspended in HPLC-grade water and centrifuged four times under the same conditions to increase the purity of peptide β-lg f1−8 in the final precipitate. The purified β-lg f1−8 peptide preparation was freeze-dried and stored at −20 °C. Taking into account that the degree of purity of the peptide in freeze-dried powder was 94.4%, as estimated from RP-HPLC chromatograms, and a molecular mass of 933.17 g/mol as obtained from the SwissProt database (http://www.expasy.org/sprot), it was calculated that 1.0 mg/mL was equivalent to 1.01 mM. However, for the sake of clarity, all of the concentration data are reported as milligrams per milliliter throughout the paper.

Solubility of Peptide β-lg f1−8 as a Function of pH and Concentration. Purified peptide β-lg f1−8 was rehydrated in HPLC-grade water, the pH was adjusted to the desired value (between 1.0 and 11.0) using HCl or NaOH, and the solutions were agitated for 1 h at room temperature. Peptide solutions were prepared at final concentrations varying from 0.5 to 50 mg/mL.

Transmission Electron Microscopy. Peptide β-lg f1−8 solutions were prepared in HPLC-grade water at a final concentration of 0.4 mg/mL, and the solutions were agitated for 1 h. The pH of solutions was adjusted by using NaOH or HCl, and the added amounts were taken into account in the calculation of the final peptide concentration. Samples (2 μL) were applied to carbon-coated copper grid, air-dried, then negatively stained with 2 μL of 1% uranyl acetate solution, and further air-dried. Specimens were examined with a JEM 1230 transmission electron microscope (JEOL, Tokyo, Japan) at 80 kV accelerating voltage. Image capture was made with a Gatan digital imaging camera and software (Gatan, Pleasanton, CA), and data analysis was performed with Image J software (http://rsbweb.nih.gov/ij/). In all cases, a minimum of 15 measurements (length and diameter) were made by selecting nanostrutures to reflect the dispersity obtained. Errors correspond to the standard deviation calculated using Excel software.

Circular Dichroism Spectroscopy. Analyses were performed using a Jasco J-710 instrument (upgraded to a J-715 with 1.08.01 spectral management software) with freshly prepared aqueous solutions of β-lg f1−8 peptide. Solubilization of peptide β-lg f1−8 was facilitated by the addition of 10% (v/v) of 2,2,2-trifluoroethanol (TFE) and 20 min of ultrasonic treatment. Solutions were made by solubilizing the required peptide amount in aqueous solution at pH 10 followed by the addition of TFE to reach 10% and 15 min of sonication. Spectra were recorded at 22 °C in a quartz cylindrical cell with a 0.01 cm path length. Ten scans were collected from 250 to 190 nm with a data pitch of 0.2 nm and a scanning speed of 100 nm/min.

The calculation of mean residual molar ellipticity (θ) (deg cm^2 dmol^{-1}) was achieved using the formula

$$(\theta) = \frac{\theta}{(10 \times C_r \times l)} \quad (1)$$

where θ = ellipticity (mdeg), C_r = mean residue molar concentration (mol/L), and l = path length of cell (cm). In turn, C_r was determined using

$$C_r = \frac{1000 \times n \times C'}{M} \quad (2)$$

where n = number of residue, C' = weighing weight (g/mL), and M = molecular weight (g/mol).

All CD measurements were duplicated. The resulting data were background-corrected and smoothed using Jasco SpectraManager software by the means-movement method with a convolution width of 15. The proportion of β-sheet content was estimated from the intensity of the negative band at 215−220 nm. A more quantitative value was obtained using DichroWeb freeware (*19*, *20*).

Solutions for CD recordings with buffered solutions were prepared by solubilizing peptide directly into 20 mM buffer solutions, incubating for 3 h, and sonicating for 15 min. For peptide concentration studies, the CD analyses were done at pH 10.0 because previous work showed that the secondary structure transition to β-sheet conformation occurs in the pH range of 9.0−11.0 (*18*). For all CD experiments, pH adjustments were achieved using NaOH and HCl solutions. The volumes added for pH adjustments were taken into account in the calculation of the final peptide concentration. The temperature-dependent spectra were recorded with a step size of 1 °C/min, with 10 scans every 10 °C and an equilibration time of 2 min before each spectrum was recorded. For the effect of dilution, stock solutions of 2.0, 1.5, and 1.0 mg/mL were prepared, and all were diluted to a final peptide concentration of 0.4 mg/mL. For the CD measurements in the presence of salt, 500 μL of the stock solution of peptide β-lg f1−8 at 4 mg/mL was mixed with 500 μL of a NaCl solution that had a concentration 2 times more concentrated than needed.

RESULTS

Effect of pH on the Solubilization of Peptide β-lg f1−8 at Various Concentrations. As summarized in **Table 1**, a clear solution was obtained at pH 1.0 and 2.0 for all of the peptide concentrations studied. However, at higher pH values, a critical peptide concentration value of ∼2.5 mg/mL was noted. Below 2.5 mg/mL of peptides, a cloudy suspension was obtained at all pH values between 3.0 and 11.0. At ≥2.5 mg/mL, a flocculated suspension was observed between pH 3.0 and 8.0, whereas hydrogels were formed at solution pH values of 9.0−11.0. At pH 10.0 and concentrations of 3−30 mg/mL, peptide β-lg f1−8 formed a soft, opalescent, self-supporting hydrogel within 2 days, whereas at a higher peptide concentration (> 50 mg/mL), a stiff and opaque hydrogel was formed instantly after pH adjustment.

Table 1. Changes in Visual Appearance of Peptide β-lg f1−8 Solutions (<2.5 mg/mL or ≥2.5 mg/mL) as a Function of pH

	pH										
peptide concn	1	2	3	4	5	6	7	8	9	10	11
< 2.5 mg/mL	clear solution	solution gets cloudy									
≥ 2.5 mg/mL	clear solution	flocculated suspension forms							hydrogel forms		

Microstructural Changes of Peptide β-lg f1−8 Suspensions as a Function of pH. Figure 1 shows transmission electron micrographs of the microstructure of peptide β-lg f1−8 solutions (0.4 mg/mL) between pH values of 2.0 and 11.0. Dimensions and morphological characteristics of the nanostructures obtained at different pH values are summarized in **Table 2**. Electron micrographs showed that, at pH 2.0 (**Figure 1a**), the peptide forms compact amorphous aggregates, consistent with the absence of any particular gel at such low pH. However, at pH 4.0 (**Figure 1b**), some fibrous aggregates could be distinguished and two types of structures are apparent; defined fibers with an average 130 nm length and 9 nm diameter were mixed with larger bundles of average 290 nm length and 35 nm diameter. At pH 6.0, fibers of approximately the same diameter (8 ± 2 nm) were observed, but

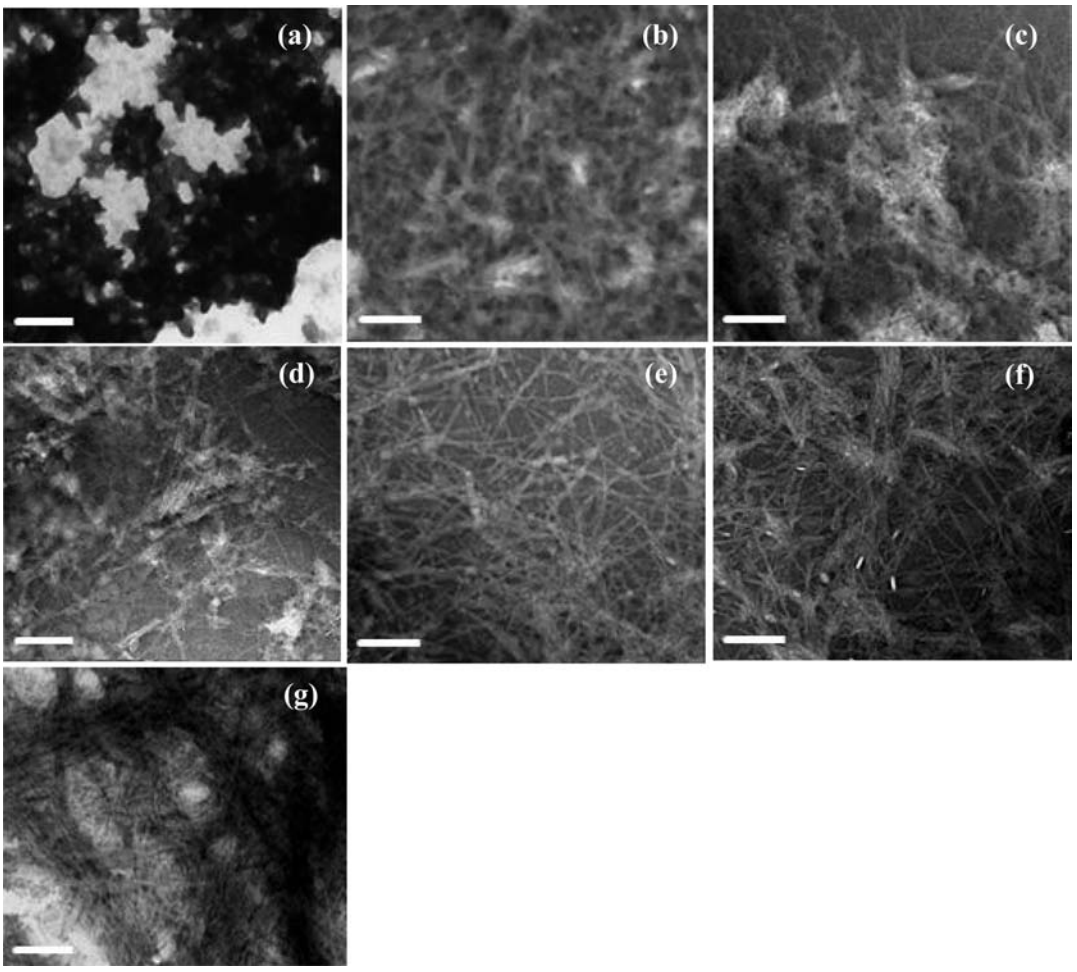

Figure 1. Transmission electron micrographs of nanostructures formed in peptide β-lg f1−8 solutions (0.4 mg/mL) at pH 2.0 (**a**), 4.0 (**b**), 6.0 (**c**), 8.0 (**d**), 9.0 (**e**), 10.0 (**f**), and 11.0 (**g**) (bars = 200 nm).

Table 2. Characteristics of Nanostructures Formed by Peptide β-lg f1−8 Solutions (0.4 mg/mL) at Different pH Values As Observed by TEM

pH	morphology	av length[a] (nm ± SD)	av diameter[a] (nm ± SD)
2	aggregates		
4	fibers	130 ± 29	9 ± 2
	bundles	290 ± 64	35 ± 5
6	fibers	659 ± 170	8 ± 2
8	fibers	356 ± 92	10 ± 2
9	fibers	483 ± 148	13 ± 4
10	fibers	225 ± 61	9 ± 4
11	fibers	nd[b]	9 ± 2

[a] Quantitative data obtained using Image J software (http://rsbweb.nih.gov/ij/). [b] No length could be measured accurately due to the significant entanglement of the fibers network.

with the difference that they are, on average, much longer (659 ± 170 nm; **Figure 1c**). The same type of fibrous assemblies was observed at pH 8 with a much shorter average length (356 nm).

At pH 9.0 (**Figure 1e**), the electron micrographs revealed a network of well-defined fibers randomly entangled. They are long on average (483 nm) and have an average diameter (13 nm) larger than all fibers observed with peptide β-lg f1−8 at other pH values.

Electron micrographs showed more fibers at pH 10.0 in comparison to pH 9.0, and defined assemblies of fibers appeared (**Figure 1f**). On average, fibers formed at pH 10.0 have a length of 225 nm and diameter of 9 nm. At pH 11.0 (**Figure 1g**), long fibers form with the same average diameter as those observed at other pH values except pH 9.0. However, the fibers are more densely packed and the network morphology is less defined, rendering accurate length measurements impossible.

It is important to note that in all cases the length distribution is broad (**Table 2**), but the average diameter of the fibers formed by peptide β-lg f1−8 is approximately 9 nm, with the exception of fibers obtained at pH 9 having a diameter of 13 nm (±4 nm). Nevertheless, by taking into account the significant distribution of fiber diameters obtained at pH 9, it is reasonable to propose that peptide β-lg f1−8 forms fibers with the same general structure at all pH values and that they differ in the length and degree of entanglement. Fibrous supramolecular assemblies formed by peptide β-lg f1−8 are reminiscent of the β-sheet nanotapes made from an 11-residue peptide and longer peptides (*21*, *22*).

Effect of Physicochemical Changes on the Secondary Structure of Peptide β-lg f1−8. *Concentration*. Changes in the proportion of β-lg f1−8 under β-sheet conformation as a function of concentration (between 0.4 and 2.0 mg/mL) were studied by CD spectroscopy. The results obtained from the CD spectra (not shown) are summarized in **Figure 2**. It can be seen that at a concentration between 0.4 and 1.0 mg/mL peptide β-lg f1−8 adopts mostly a random coil conformation. At concentrations between 1.0 and 1.5 mg/mL, solutions contained a mixture of peptide units as random coils and β-sheet conformations in various proportions. Thus, the CD results support the hypothesis that self-assembly of peptide β-lg f1−8 is concentration-dependent in the range studied.

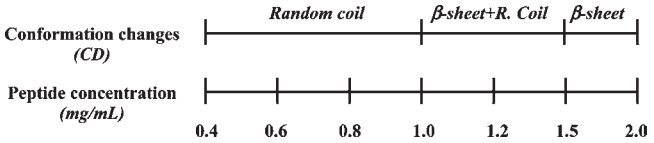

Figure 2. Summary of conformation changes in peptide β-lg f1−8 solutions at pH 10.0 as a function of final peptide concentrations varying from 0.4 to 2 mg/mL, as determined by CD spectroscopy.

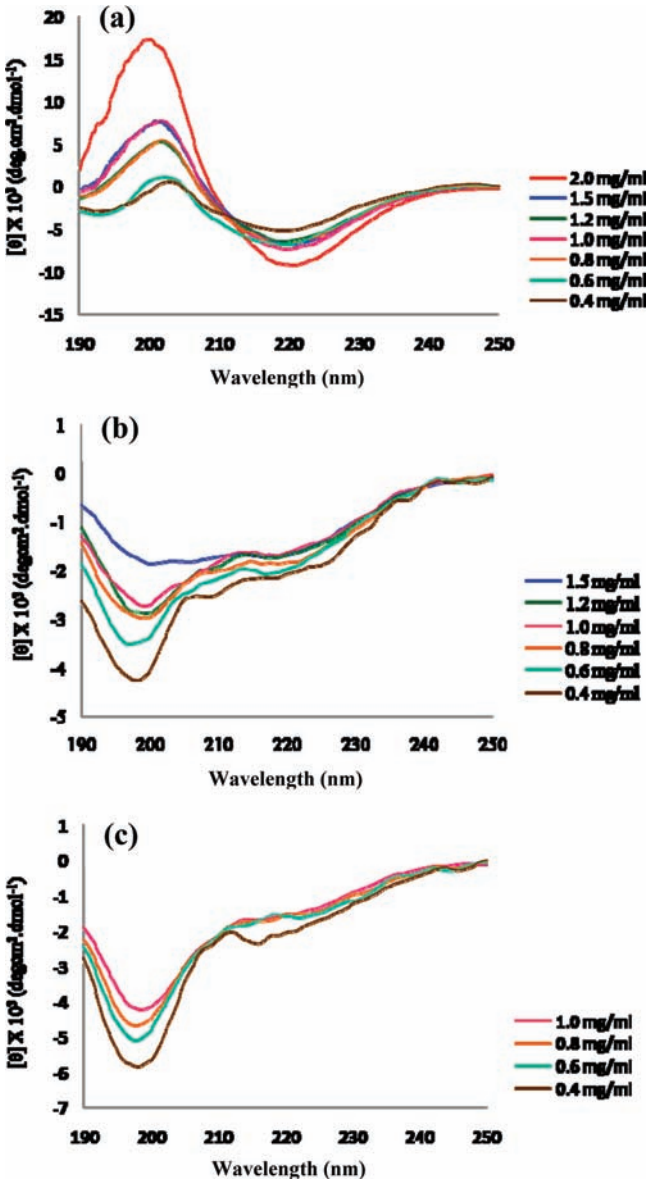

Figure 3. CD spectra of peptide β-lg f1−8 aqueous solutions at pH 10.0 and final peptide concentrations of 2.0 mg/mL (**a**), 1.5 mg/mL (**b**), and 1.0 mg/mL (**c**) and their respective diluted solutions until a final peptide concentration of 0.4 mg/mL.

CD analyses were also performed to determine the stability of the conformations adopted by peptide β-lg f1−8 as a function of the concentration. **Figure 3** shows CD spectra of stock solutions, respectively, at 2.0 (**a**), 1.5 (**b**), and 1.0 mg/mL (**c**), all diluted to a final peptide concentration of 0.4 mg/mL. The results showed that the stock solution of 2.0 mg/mL (**Figure 3a**) displayed a typical β-sheet pattern, which was maintained upon dilution. The 1.5 mg/mL stock solution (**Figure 3b**) initially displayed a curve with two small negative minima around 220 and 200 nm,

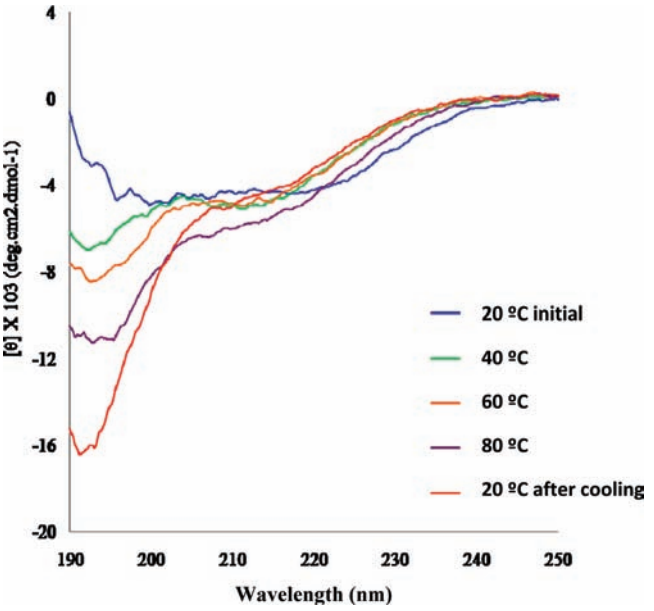

Figure 4. Temperature-dependent CD spectra recorded from 20 to 80 °C and then cooled to 20 °C for peptide β-lg f1−8 aqueous solutions at pH 10 at a final peptide concentration of 1.5 mg/mL.

indicative of a mix of β-sheet and random coil conformations, which upon dilution gradually changed for a greater minimum around 200 nm, associated with an increase of peptide units under a random coil conformation. The 1.0 mg/mL stock solution (**Figure 3c**) displayed a CD spectrum with a small minimum around 220 nm and a more significant minimum around 200 nm, indicative of a random coil conformation with a small amount of peptide units under β-sheet conformation, and this characteristic pattern was preserved upon dilution.

Temperature. The effect of temperature on the stability of peptide β-lg f1−8 was monitored in a range between 20 and 80 °C using CD spectroscopy (**Figure 4**). The CD spectrum at 20 °C before heating showed two negative minima, one around 220 nm and a smaller one around 200 nm, which indicates that peptide β-lg f1−8 initially adopts mainly a β-sheet conformation with a small amount of peptide units in a random coil conformation. A similar CD spectrum was obtained at 40 °C with a minimum around 216 nm and a minimum around 195 nm, which is typical of random coil conformation. No major changes in the secondary structure were observed between 40 and 60 °C, except for a small increase of the signal due to random coil conformation. When the maximum temperature (80 °C) for the CD experiments was reached, results showed an important increase in the signal for both β-sheet and random coil conformations. This observation highlights that changes observed in the spectra at 60 and 80 °C are not due to an alteration of the secondary structures adopted by peptide β-lg f1−8 but are probably associated with an increase of peptide solubility upon heating.

When the sample was then cooled to 20 °C, the resulting CD spectrum displayed a minimum around 216 nm of the same intensity observed at 20, 40, and 60 °C and an important minimum around 195 nm. These results suggest that the ratio of peptide units folded into β-sheet versus peptide units under random coil conformation decreases after a heating−cooling cycle.

Ionic Strength and Buffer System. CD analyses were performed at pH 6.5, below the optimal pH value for β-sheet formation (pH 10.0), to check if self-assembly of peptide β-lg f1−8 can be triggered at a different pH value by adding salts.

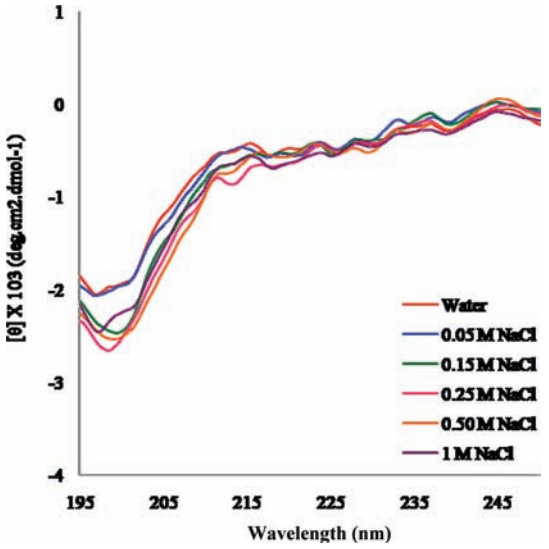

Figure 5. CD spectra of peptide β-lg f1−8 aqueous solutions at pH 6.5 and a final peptide concentration of 2.0 mg/mL in the presence of various concentrations of NaCl (0−1.0 M).

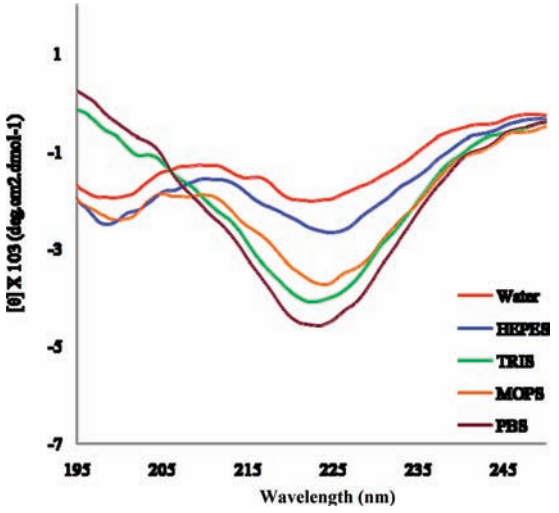

Figure 6. CD spectra of peptide β-lg f1−8 solutions at pH 8.0 at a final peptide concentration of 2.0 mg/mL. The peptide solutions were prepared either in HPLC water or in buffer solutions (20 mM).

Increasing the ionic strength of the solution by adding up to 1 M NaCl led to a slight increase in the negative band centered at 200 nm associated with random coil structures (**Figure 5**). However, there was no significant change in the β-sheet correlating band at 215−220 nm band, showing that aggregation was not induced in a noticeable manner.

The effect of ionic strength was also investigated using different buffered solutions to assess if ions other than Na^+Cl^- could shield the charges on peptide β-lg f1−8 more efficiently and trigger self-assembly.

Figure 6 shows CD spectra of peptide β-lg f1−8 in 20 mM aqueous solution of four different buffer solutions in comparison to HPLC-grade water as control. Peptide β-lg f1−8 was slightly more soluble in HEPES buffered solution, as the CD spectrum displayed increased signals around 220 and 195 nm. The same effect was observed in the MOPS buffer with a greater increase of the β-sheet signal around 220 nm. The CD spectra in Tris and PBS buffers both displayed similar curves with the same signal intensity around 220 nm as the MOPS buffer, but without the small minimum around 195 nm due to random coil conformation. Thus, results indicate that both Tris and PBS buffers could also improve peptide β-lg f1−8 solubility and promote β-sheet formation.

DISCUSSION

Hydrogel formation was not observed in our previous work (*18*) because the concentration used for CD measurements was below the critical gelation concentration of 2.5 mg/mL that we have determined in the present study. The kinetics of hydrogel formation depends heavily on peptide concentration, as hydrogels are formed within a few seconds at higher peptide concentrations and only after a few days when the peptide concentration is low. On the other hand, electron micrographs obtained between pH 4.0 and 10.0 suggest that peptide β-lg f1−8 undergoes a one-dimensional self-assembly process, characterized by aggregate growth in only one dimension, whereas the other dimensions remain constant (*21*−*24*). Micrographs and CD results at pH values of 9.0 and 10.0 suggest that the fiber network formed resulted from a self-assembly of peptide β-lg f1−8 units mainly under a β-sheet conformation. This is further supported by recent reviews describing the structural analysis of peptides that use β-structures to assemble to form filaments, fibrils, and long fibrous structures (*15*, *16*).

The impact of pH on hydrogel formation is likely to be driven by changes in charge distribution on the peptide β-lg f1−8 as a function of pH. As seen in **Table 3**, two transitions in the charges carried by peptide β-lg f1−8 occur in the pH range where hydrogel formation has been observed. First, the N-terminal group of the peptide loses its positive charge at pH 9.6, and, second, the lysine side chain loses its positive charge at pH 10.5. A number of studies (*2*,*8*,*10*,*11*,*25*,*26*) showed that peptide folding and self-assembly are contingent upon elimination of charge repulsion between neighboring lysine residues via deprotonation at high pH (*12*). Also, a similar phenomenon with a peptide containing a glutamic acid residue showed that, as pH is increased, more glutamic acid side chains are deprotonated and the repulsions between peptide chains increase further, giving higher proportions of peptide molecules under a monomeric state (*27*). Thus, a decrease in the repulsive electrostatic interactions between neighboring side chains allows peptide units to get closer, improves productive intermolecular interactions between peptide backbones, and favors β-sheet formation. Therefore, the optimal hydrogel formation by peptide β-lg f1−8 observed at pH 10 might be the result of an optimal repulsion−attraction balance between neighboring peptide side chains occurring when both the N-terminal group and lysine side chain lose their positive charge around pH 10.0.

Another important transition in charges carried by peptide β-lg f1−8 occurs at pH 2.2, at which the C-terminal group of the peptide becomes negatively charged while both the N-terminal and lysine side chain are positively charged, a condition associated with the transition from a clear solution to a flocculate solution between pH 2.0 and 3.0. The negative charge arising from the C-terminal end of peptide β-lg f1−8 probably favors peptide−peptide interactions that result in random aggregation of peptide units into a light flocculate.

Peptide concentration had a significant effect on the conformational equilibrium of peptide β-lg f1−8. This is possible as a higher concentration favors peptide−peptide interaction and the formation of defined supramolecular aggregates. Therefore, at 2 mg/mL, a large proportion of the peptide molecules in solution exist as supramolecular aggregates with the backbone under a β-sheet conformation. At lower concentration, more peptide

Table 3. Structural Characteristics and Interaction Potential of Peptide β-Lg f1−8 as a Function of pH[a]

pH	Ionization State	Charge distribution[1]	Secondary Structure[2]	Peptide interactions
1	I	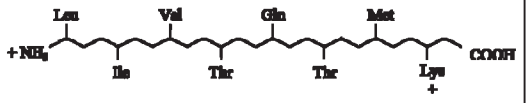	Random coil	*Maximal repulsions (protonated)*
2				
3	II	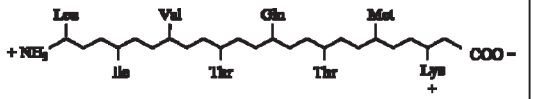		*Electrostatic interactions/ Aggregation*
4				
5				
6				
7				
8				
9			β-sheets	*Optimal attractions/ repulsions between monomeric peptides*
10	III	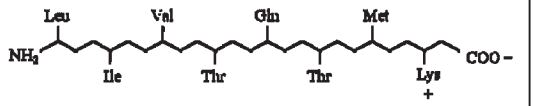		
11	IV	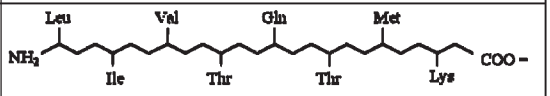		

[a] [1] p*K* values for ionizations are 2.2 (II), 9.6 (III), and 10.5 (IV). [2] As determined by CD in Pouliot et al. (*18*) at a concentration of 0.4 mg/mL.

molecules are free and structureless (random coil) than involved in structured aggregates because it can be triggered when the right peptide concentration (2.0 mg/mL) is reached and disfavored at low peptide concentration.

Our CD measurements on different dilutions of stock solutions demonstrate that the secondary structure adopted by peptide β-lg f1−8 exhibits a greater stability only when the peptide is mostly folded into a β-sheet. Hence, the self-assembled supramolecular structure formed at 2.0 mg/mL is more stable and maintains its β-sheet conformation even upon dilution. In peptide self-assembly models, the transition from one structure to the next higher order structure occurs at a set of well-defined critical concentrations, above which the size and concentration of the lower order structure are fixed (*24*). Hence, for the self-assembly of peptide β-lg f1−8, the critical concentration of β-sheet formation is 2.0 mg/mL and the critical concentration for hydrogel formation is 2.5 mg/mL.

The effect of temperature on the CD measurements demonstrates that temperature is not a significant physicochemical parameter in the β-sheet formation and self-assembly of peptide β-lg f1−8. Also, CD results highlight that peptide β-lg f1−8 is significantly heat stable as the peptide remains folded into a β-sheet form even after heating to 80 °C and cooling to 20 °C . It seems that an additional portion of peptide units solubilized upon heating, and these existed as random coil structures during cooling, leading to an increase of the random coil signal after cooling to 20 °C.

From literature precedents, we expected that raising the ionic strength of the peptide solution would decrease the electrostatic repulsions between charged residues, promote β-sheet formation, and therefore trigger peptide self-assembly. Indeed, it has been suggested that the self-assembly of peptides can be triggered by adding NaCl (*24*, *25*, *27*−*29*). As charge−charge interactions are involved in peptide self-assembly, salt concentration could potentially affect the assembly of these systems by masking the charges involved in the interactions between multiple strands and sheets (*15*). However, our data do not support this view. As seen in **Figure 5**, the conformation of peptide β-lg f1−8 remains unchanged in NaCl solutions in the range of concentrations used, from 0.5 to 1 M. Furthermore, CD measurements in different buffer solutions (**Figure 6**) indicate that no major structural transition of peptide β-lg f1−8 was triggered, as the negative

band at around 220 nm does not shift. However, buffer solutions can be a useful tool to improve solubility and to increase the proportion of peptide units that adopt a β-sheet conformation, as observed by the increased ellipticity of the characteristic band in the 215−220 nm region.

Overall, our results suggest that the self-assembly of peptide β-lg f1−8 occurs via a hierarchical and well-ordered mechanism. Nanofiber and hydrogel formation processes are fully dependent on the conformational state of the peptide, implying a direct relationship between β-sheet formation (as measured by CD spectropolarimetry) and the evolution of hydrogel structure (*30*).

ACKNOWLEDGMENT

We thank Alain Goulet for technical support in TEM analysis.

LITERATURE CITED

(1) Colombo, G.; Soto, P.; Gazit, E. Peptide self-assembly at the nanoscale: a challenging target for computational and experimental biotechnology. *Trends Biotechnol*. **2007**, *25* (5), 211−218.

(2) Haines-Butterick, L.; Rajagopal, K.; Branco, M.; Salick, D. A.; Rughani, R.; Pilarz, M.; Lamm, M.; Pochan, D. J.; Schneider, J. P. Controlling hydrogelation kinetics by peptide design for three-dimensional encapsulation and injectable delivery of cells. *Proc. Natl. Acad. Sci. U.S.A*. **2007**, *104* (19), 7791−7796.

(3) Holmes, T. C.; De Lacalle, S.; Su, X.; Liu, G.; Rich, A.; Zhang, S. Extensive neurite outgrowth and active synapse formation on self-assembling peptide scaffolds. *Proc. Natl. Acad. Sci. U.S.A*. **2000**, *97* (12), 6728−6733.

(4) Kirkham, J.; Firth, A.; Vernals, D.; Boden, N.; Robinson, C.; Shore, R. C.; Brookes, S. J.; Aggeli, A. Self-assembling peptide scaffolds promote enamel remineralization. *J. Dental Res*. **2007**, *86* (5), 426−430.

(5) Rajangam, K.; Arnold, M. S.; Rocco, M. A.; Stupp, S. I. Peptide amphiphile nanostructure−heparin interactions and their relationship to bioactivity. *Biomaterials* **2008**, *29*, 3298−3305.

(6) Reches, M.; Gazit, E. Molecular self-assembly of peptide nanostructures: mechanism of association and potential uses. *Curr. Nanosci*. **2006**, *2*, 105−111.

(7) Aggeli, A.; Nyrkova, I. A.; Bell, M.; Harding, R.; Carrick, L.; Mcleish, T. C. B.; Semenov, A. N.; Boden, N. Hierarchical self-assembly of chiral rod-like molecules as a model for peptide β-sheet tapes, ribbons, fibrils, and fibers. *Proc. Natl. Acad. Sci. U.S.A*. **2001**, *98* (21), 11857−11862.

(8) Kretsinger, J.; Haines, L. A.; Ozbas, B.; Pochan, D. J.; Schneider, J. P. Cytocompatibility of self-assembled β-hairpin peptide hydrogel surfaces. *Biomaterials* **2005**, *26*, 5177−5186.

(9) Otte, J.; Ipsen, R.; Bauer, R.; Bjerrum, M. J.; Waninge, R. Formation of amyloid-like fibrils upon limited proteolysis of bovine α-lactalbumin. *Int. Dairy J*. **2005**, *15*, 219−229.

(10) Rajagopal, K.; Ozbas, B.; Pochan, D. J.; Schneider, J. P. Probing the importance of lateral hydrophobic association in self-assembling peptide hydrogelators. *Eur. Biophys. J*. **2006**, *35*, 162−169.

(11) Salick, D.; Kretsinger, J. K.; Pochan, D. J.; Schneider, J. P. Inherent antibacterial activity of a peptide-based β-hairpin hydrogel. *J. Am. Chem. Soc*. **2007**, *129*, 14793−14799.

(12) Schneider, J. P.; Pochan, D. J.; Ozbas, B.; Rajagopal, K.; Pakstis, L.; Kretsinger, J. Responsive hydrogels from the intramolecular folding and self-assembly of a designed peptide. *J. Am. Chem. Soc*. **2002**, *124*, 15030−15037.

(13) Tuchscherer, G.; Chandravarkar, A.; Camus, M.-S.; Bérard, J.; Murat, K.; Schmid, A.; Mimna, R.; Lashuel, H. A.; Mutter, M. Switch-peptides as folding precursors in self-assembling peptides and amyloid fibrillogenesis. *Biopolymers* **2007**, *88* (2), 239−252.

(14) Wang, C.; Huang, L.; Wang, L.; Hong, Y.; Sha, Y. One-dimensional self-assembly of a rational designed β-structure peptide. *Biopolymers* **2007**, *86*, 23−31.

(15) Ulijn, R. V.; Smith, A. M. Designing peptide based nanomaterials. *Chem. Soc. Rev*. **2008**, *37*, 664−675.

(16) Fairman, R.; Åkerfeldt, K. S. Peptides as novel smart materials. *Curr. Opin. Struct. Biol*. **2005**, *15*, 453−463.

(17) Ipsen, R.; Otte, J.; Qvist, K. B. Molecular self-assembly of partially hydrolysed α-lactalbumin resulting in strong gels with a novel microstructure. *J. Dairy Res*. **2001**, *68*, 277−286.

(18) Pouliot, Y.; Guy, M.-M.; Tremblay, M.; Gaonac'h, A.-C.; Chay Pak Ting, B. P.; Gauthier, S. F.; Voyer, N. Isolation and characterization of an aggregating peptide from a tryptic hydrolysate of whey proteins. *J. Agric. Food Chem*. **2009**, *57*, 3760−3764.

(19) Whitmore, L.; Wallace, B. A. Protein secondary structure analyses from circular dichroism spectroscopy: methods and reference databases. *Biopolymers* **2008**, *89*, 392−400.

(20) Whitmore, L.; Wallace, B. A. DICHROWEB, an online server for protein secondary structure analyses from circular dichroism spectroscopic data. *Nucleic Acids Res*. **2004**, *32*, W668−W673.

(21) Davies, R. P. W.; Aggeli, A.; Beevers, A. J.; Boden, N.; Carrick, L. M.; Fishwick, C. W. G.; McLeish, T. C. B.; Nyrkova, I.; Semenov, A. N. Self-assembling β-sheet tape forming peptides. *Supramol. Chem*. **2006**, *18*, 435−443.

(22) Aggeli, A.; et al. Responsive gels formed by the spontaneous self-assembly of peptides into polymeric ss-sheet tapes. *Nature* **1997**, *386*, 259−262.

(23) Aggeli, A.; et al. Engineering peptide β-sheet nanotapes. *J. Mater. Chem*. **1997**, *7*, 1135−1146.

(24) Aggeli, A.; Bell, M.; Carrick, L. M.; Fishwick, C. W. G.; Harding, R.; Mawer, P. J.; Radford, S. E.; Strong, A .E.; Boden, N. pH as trigger of peptide β-sheet self-assembly and reversible switching between nematic and isotropic phases. *J. Am. Chem. Soc*. **2003**, *125*, 9619−9628.

(25) Dong, H.; Paramonov, S. E.; Aulisa, L.; Bakota, E. L.; Hartgerink, J. D. Self-assembly of multidomain peptides: balancing molecular frustration controls conformation and nanostructures. *J. Am. Chem. Soc*. **2007**, *129*, 12468−12472.

(26) Lamm, M. S.; Rajagopal, K.; Schneider, J. P.; Pochan, D. J. Laminated morphology of nontwisting β-sheet fribrils constructed via peptide self-assembly. *J. Am. Chem. Soc*. **2005**, *127*, 16692−16700.

(27) Carrick, L. M.; Aggeli, A.; Boden, N.; Fisher, J.; Ingham, E.; Waigh, T. A. Effect of ionic strength on the self-assembly, morphology and gelation of pH responsive β-sheet tape-forming peptides. *Tetrahedron* **2007**, *63*, 7457−7467.

(28) Veerman, C.; Rajagopal, K.; Palla, C. S.; Pochan, D. J.; Schneider, J. P.; Furst, E. M. Gelation kinetics of β-hairpin peptide hydrogel networks. *Macromolecules* **2006**, *39*, 6608−6614.

(29) Zhang, S.; Holmes, T.; Lockshin, C.; Rich, A. Spontaneous assembly of a self-complementary oligopeptide to form a stable macroscopic membrane. *Proc. Natl. Acad. Sci. U.S.A*. **1993**, *90*, 3334−3338.

(30) Creighton, T. E. *Proteins: Structures and Molecular Properties*, 2nd ed.; Freeman: New York, 1993.

Received for review August 26, 2010. Revised manuscript received November 30, 2010. Accepted December 6, 2010. This work was supported by grants from the Natural Sciences and Engineering Research Council of Canada (NSERC) and by the Fonds Québécois de la Recherche sur la Nature et les Technologies (FQRNT). M.-M.G. thanks the Quebec Protein Structure, Function and Engineering Research Network (PROTEO) for an international travel award.